

# Sequence-Encoded Self-Assembly of Multiple-Nanocomponent Arrays by 2D DNA Scaffolding

Yariv Y. Pinto,<sup>†,‡</sup> John D. Le,<sup>†</sup> Nadrian C. Seeman,<sup>§</sup> Karin Musier-Forsyth,<sup>‡</sup> T. Andrew Taton,<sup>‡</sup> and Richard A. Kiehl<sup>\*,†</sup>

*Department of Electrical and Computer Engineering and Department of Chemistry, University of Minnesota, Minneapolis, Minnesota 55455, and Department of Chemistry, New York University, New York, New York 10003*

*Received August 7, 2005; Revised Manuscript Received October 11, 2005*

## ABSTRACT

Regular 2D arrays of multiple types of nanocomponents were constructed by self-assembly to DNA scaffolding with alternating rows of sequence-encoded hybridization sites. Different-sized Au particles coated with DNA complementary to one of the sites were bound to the scaffolding, producing alternating rows of the two nanocomponents with a 32-nm inter-row spacing. These results demonstrate the potential for using DNA to self-assemble complex arrays of components with nanometer-scale precision.

The predictability of Watson–Crick base-pair association and the structural rigidity of modular DNA assembly units, such as double-crossover (DX) molecules, are useful for assembling nanometer-scale components into programmable arrangements with high precision. Although RNA<sup>1</sup>- and protein-based<sup>2</sup> molecular self-assembly offer the structural and functional diversity needed for biological applications such as tissue engineering, the predictability and rigidity of DNA scaffolding are advantageous for applications demanding a high degree of structural control and accuracy. The assembly of nanoscale circuitry is an example of such an application. Nanoelectronic and nanophotonic circuitry based on arrays of nanoparticles<sup>3,4</sup> will require the layout of multiple types of components in regular 2D arrangements at the nanometer scale.

Recently, we<sup>5</sup> and others<sup>6</sup> demonstrated that a 2D scaffolding composed of DNA molecules, first reported by Seeman and co-workers,<sup>7</sup> could be used to arrange a single type of gold nanocomponent into regular rows with nanometer-scale spatial control. By using a two-step assembly scheme on a surface, we were able to fabricate regular arrays over micrometer-scale areas.<sup>5</sup> In those studies, the assembly of the nanocomponents was dictated by hybridization of nanoparticle-bound, single-stranded DNA to complementary DNA sequences at predetermined locations on the array. Here

we demonstrate that this principle can be extended to the precise arrangement of multiple, DNA-encoded nanocomponents, in which the location of each component is determined by selective hybridization of its encoding strand to a complementary capture sequence at a specific location on the DNA scaffolding.

The scaffolding used in this study consists of four different double-crossover DNA “tiles” (Figure 1) that assemble spontaneously into a regular 2D structure. The basic structure of the scaffolding is similar to systems published previously,<sup>5,7</sup> except that different single-strand sequences protrude from tiles B and D for nanocomponent attachment. These single-stranded attachment sites were designed to project out of the same face of the scaffolding. Au nanoparticles with diameters of 10 and 5 nm were then functionalized with single-stranded 3'-thiol-modified DNA molecules that were designed to complement the B- and D-tile attachment sequences, respectively. In this design, the other two tiles (A and C) dictate a spatial separation of 32 nm between the B- and D-component rows. As a result, the scaffolding is designed to assemble alternating rows of equally spaced large and small particles. In addition, tile D incorporated a hairpin structure (on the opposite face of the array from the particles) as a topological marker for verifying the initial assembly of the array.

The directed self-assembly of the arrays of two types of nanocomponents was performed in several steps (Figure 2). First, the DNA scaffolding was preassembled in solution by annealing a mixture of stoichiometric quantities of the constituent oligonucleotides in buffer, as described previ-

\* To whom correspondence should be addressed. E-mail: kiehl@ece.umn.edu.

<sup>†</sup> Department of Electrical and Computer Engineering, University of Minnesota.

<sup>‡</sup> Department of Chemistry, University of Minnesota.

<sup>§</sup> Department of Chemistry, New York University.

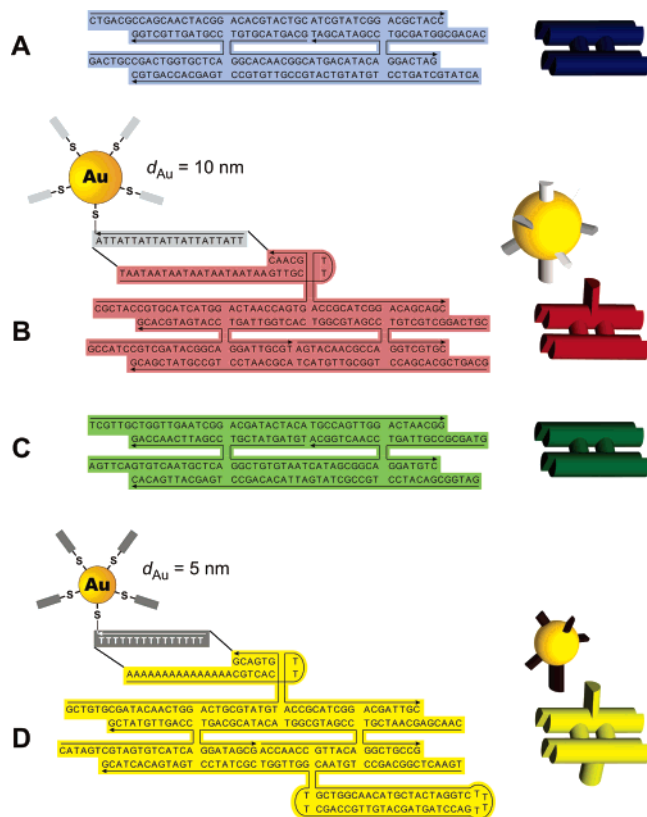


**Figure 1.** Base sequences and geometric arrangements of the DX subunits and DNA–Au nanocomponents. A unique color is chosen for each DX tile type and corresponds to that used in the illustration of the assembled scaffolding (Figure 2). Arrowheads indicate the 3' ends of the strands. Each spherical Au nanoparticle bears a shell composed of multiple identical DNA strands (typically 5–10 strands per 5-nm particle and 60–70 per 10-nm particle) that are complementary to the hybridization sites on tiles B and D. (The sequence is shown explicitly for one strand only.) A (dT)<sub>15</sub> or (dT)<sub>7</sub> shell was used for the tile D nanocomponent in these experiments; the case of (dT)<sub>15</sub> is shown.

ously.<sup>5</sup> The mixture was then deposited on mica, and the assembled scaffolds were allowed to adsorb to the surface. The sample was rinsed to remove excess DNA and salts. Atomic force microscope (AFM) topographic images (Figure 3a) of these samples show that the scaffolding exhibits alternating major and minor ridges, corresponding to the alternating rows of the two different half-hairpin attachment sites. The ridges are separated by 32 nm, the distance between B and D tiles in the scaffolding.

The scaffolding was exposed to a buffer solution of 5-nm gold particles coated with (dT)<sub>15</sub> or (dT)<sub>7</sub>. AFM images show that these nanocomponents were assembled into parallel rows with a 64-nm inter-row separation (Figure 3b). Very few of the attached particles appear to have adhered to the “wrong” row. The average gap between particles was approximately 10 nm.<sup>8</sup>

The samples were then exposed to a buffer solution of 10-nm Au nanoparticles coated with a different targeting sequence, (dTdTa)<sub>7</sub>. These nanocomponents hybridized to the other row of attachment sites (tile B). AFM images clearly show alternating rows of small and large nanocomponents (Figure 3c).<sup>9</sup>

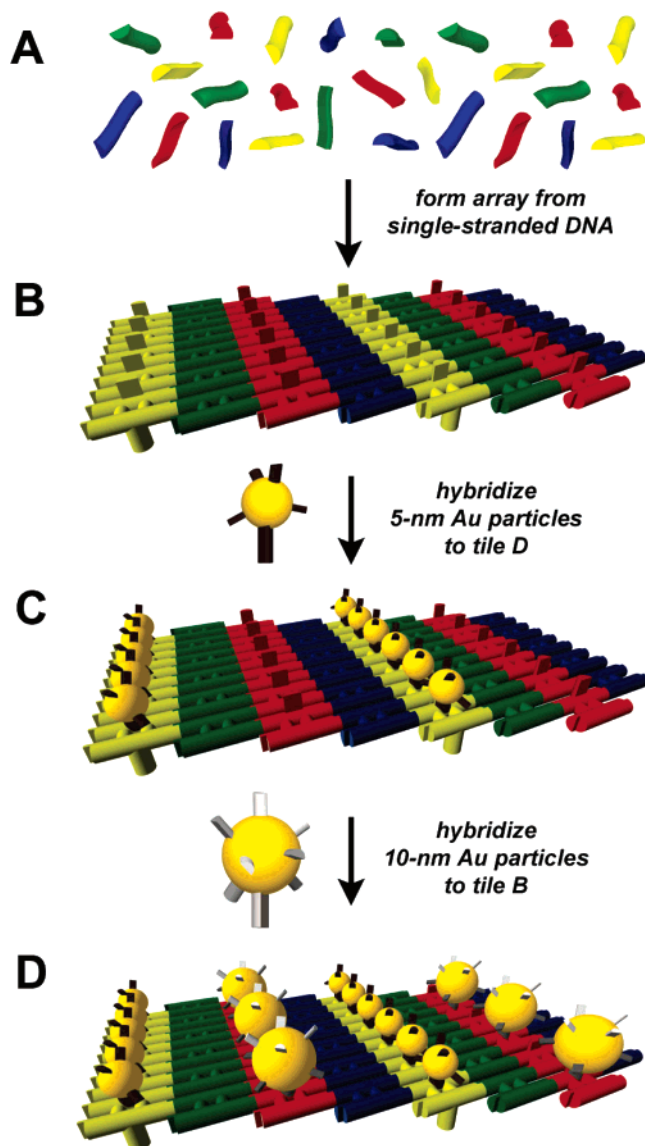


**Figure 2.** Assembly steps for the 2D nanocomponent arrays. (A) The DNA scaffolding is first assembled in solution from the set of 22 strands. (B) A suspension of the DNA scaffolding is deposited on mica, allowing the scaffolding to attach to the surface. The scaffolding is composed entirely of double-stranded DNA, except for the open single-stranded hybridization sites on the B and D tiles. (C) The scaffolding is combined with DNA-encoded nanocomponents, which attach to the open hybridization sites on tile D. (D) The second nanocomponent is attached to the open hybridization sites on tile B. Although this diagram shows one nanocomponent occupying each site, single nanoparticles can also attach to multiple sites via hybridization of multiple nanoparticle-bound strands.

Finally, the samples were imaged by TEM to allow high-resolution visualization of the Au-particle cores in the nanocomponent array. A representative TEM image (Figure 4) shows the alternating rows of the two sets of nanocomponents. The 5-nm particles are seen to be more closely packed than the 10-nm particles. The rows of smaller particles also appear straighter than the rows of larger particles. These differences may be due to the different lengths of the strands used to tether the smaller and larger particles to the scaffolding (15 and 21 nucleotides, respec-

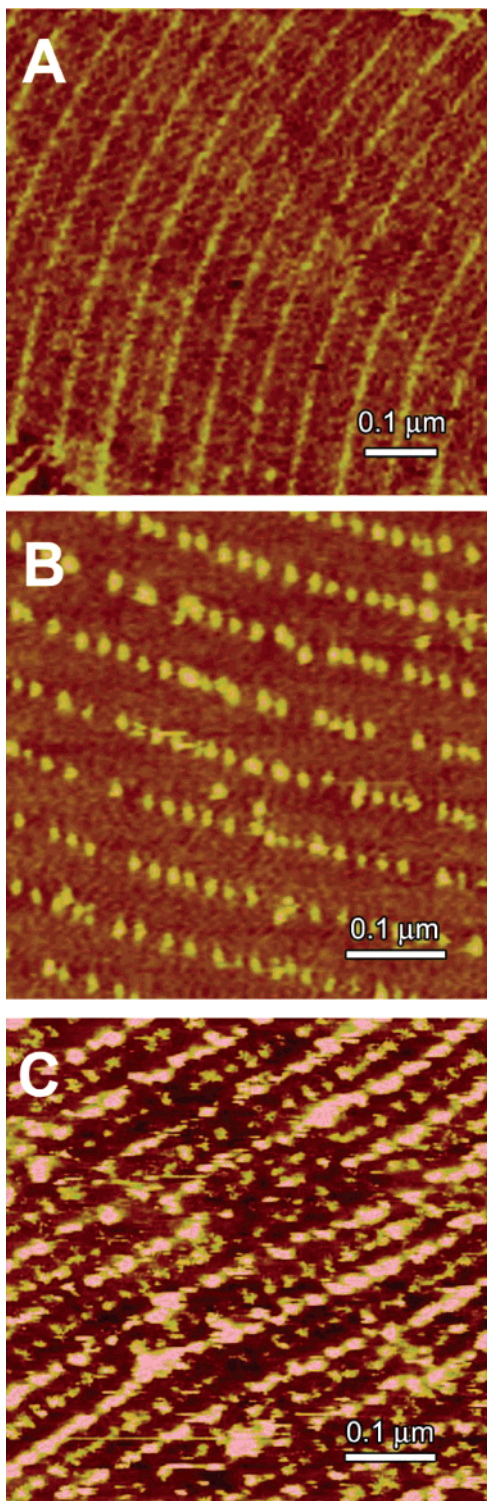


**Figure 3.** AFM images of the DNA scaffolding before, during, and after nanocomponent attachment. (A) Prior to nanocomponent attachment. The surface of the DNA scaffolding is 1.6–1.8 nm higher than the mica surface and the heights of the major and minor ridges are  $0.2 \pm 0.1$  and  $0.6 \pm 0.1$  nm above the scaffolding surface. (B) Hybridized with 5-nm (dT)<sub>7</sub>-coated Au particles. The measured height difference between the particles and the scaffolding surface is  $5.2 \pm 0.8$  nm. (C) Hybridized with both sizes of particles: 5-nm (dT)<sub>15</sub>-coated Au particles and 10-nm (dTdTdA)<sub>7</sub>-coated Au particles. Alternating parallel rows of different-sized particles are visible. The larger particles are hybridized to the tile B rows, and the smaller particles are hybridized to the rows of tile D. The repeat distance between lines of same-sized particles is 64 nm.

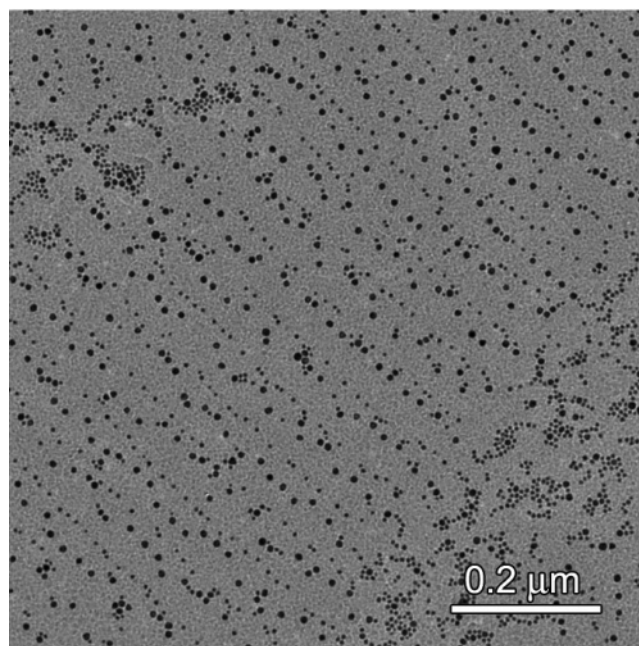


**Figure 4.** TEM image of the two-particle array. The pattern of alternating parallel rows of small and large gold particles is clearly visible. (Particles tend to aggregate on the mica surface outside the arrays, e.g., lower right corner of image.)

tively).<sup>10</sup> Importantly, the TEM image shows that there is virtually no cross-contamination of the nanocomponent rows; each particle size is found almost exclusively in its row and not the other.

In these experiments, we have succeeded in encoding the self-assembly of different nanocomponent elements by DNA base sequence. We did, however, find limitations in the types of DNA sequences that could be used to target particles to scaffolding addresses successfully. The sequences used here were made up entirely of adenosines and thymidines to limit nonspecific binding of particles to the scaffolding and mica surface. These sequences are known to have considerably less nonspecific interaction with gold surfaces than the other DNA bases.<sup>11,12</sup> Indeed, nanoparticles bearing sequences with a uniform distribution of A, T, G, and C nucleotides failed to form ordered arrays and did not adhere to complementary capture sequences on the DNA scaffolding. In this case, nonspecific interactions between the particle-bound targeting sequence and the Au particle surface may have interfered with proper hybridization to the scaffolding complements. Thymine-rich nanoparticle-shell sequences did not appear to have this effect and promoted specific over nonspecific attachment of nanocomponents to the scaffolding.

In summary, we have exploited the sequence selectivity of DNA to assemble two different types of nanocomponents into arrays on a common structure by self-assembly to a 2D DNA scaffolding. These results demonstrate the potential for the self-assembly of complex arrays of components with nanometer-scale precision. The remarkable ability to control the position of different elements in a complex structure by encoding the base sequence of the element's DNA shell is a consequence of the programmability of DNA. These results represent a critical step toward a versatile manufacturing

technology with a wide range of applications in nanomaterials, nanoelectronics, and nanomechanical systems.

**Acknowledgment.** This work was supported by NSF Nanoscale Interdisciplinary Research Team (NIRT) grant NSF/DMI-0210844.

## References

- (1) Chworos, A.; Severcan, I.; Koyfman, A. Y.; Weinkam, P.; Oroudjev, E.; Hansma, H. G.; Jaeger, L. *Science* **2004**, *306*, 2068–2072.
- (2) McMillan, R. A.; Howard, J.; Zaluzec, N. J.; Kagawa, H. K.; Mogul, R.; Li, Y.-F.; Paavola, C. D.; Trent, J. D. *J. Am. Chem. Soc.* **2005**, *127*, 2800–2801.
- (3) Kiehl, R. A. *J. Nanopart. Res.* **2000**, *2*, 331–332.
- (4) Maier, S. A.; Brongersma, M. L.; Kik, P. G.; Meltzer, S.; Requicha, A. A. G.; Atwater, H. A. *Adv. Mater.* **2001**, *13*, 1501–1505.
- (5) Le, J. D.; Pinto, Y.; Seeman, N. C.; Musier-Forsyth, K.; Taton, T. A.; Kiehl, R. A. *Nano Lett.* **2004**, *4*, 2343–2347.
- (6) Li, H.; Park, S. H.; Reif, J. H.; LaBean, T. H.; Yan, H. *J. Am. Chem. Soc.* **2004**, *126*, 418–419.
- (7) Winfree, E.; Liu, F.; Wenzler, L. A.; Seeman, N. C. *Nature* **1998**, *394*, 539–544.
- (8) The polyvalency of the ssDNA-coated Au nanoparticles allows each nanocomponent to attach to multiple hybridization sites along a row. Thus, the gap between nanocomponents along a row is governed by the length of the strands in the nanocomponent shell. The results of a separate study in which we confirmed this scaling of gap with strand length will be published elsewhere.
- (9) The amount of curvature found in the AFM images of the arrays varied considerably from one piece of scaffolding to another on the same substrate. Differences in curvature for the different panels of Figure 3 do not represent a systematic trend. We believe that the curvature is an artifact of the sample preparation caused by a stretching of the scaffolding as it adheres to the mica surface.
- (10) Arrays were also made with the reverse sizing of particles (5-nm (dTdTdA)<sub>7</sub>-coated Au and 10-nm (dT)<sub>7</sub>-coated particles). AFM imaging does not show any difference between the arrays reported and those with the reverse sizes.
- (11) Kimura-Suda, H.; Petrovykh, D. Y.; Tarlov, M. J.; Whitman, L. J. *J. Am. Chem. Soc.* **2003**, *125*, 9014–9015.
- (12) Sandstroem, P.; Boncheva, M.; Kerman, B. *Langmuir* **2003**, *19*, 7537–7543.

NL0515495